metals

Article

Electrochemical Recycling of Platinum Group Metals from Spent Catalytic Converters

Cornelia Diac[1,2], Florentina Iuliana Maxim[1,2], Radu Tirca[2], Adrian Ciocanea[3], Valeriu Filip[2], Eugeniu Vasile[4,*], and Serban N. Stamatin[1,*]

[1] 3Nano-SAE Research Centre, University of Bucharest, Bucharest 077125, Romania; cornelia.diac@3nanosae.org (C. D.); iuliana.maxim@3nanosae.org (F.I.M.); serban@3nanosae.org (S.N.S.)
[2] Faculty of Physics, University of Bucharest, Bucharest 077125, Romania; radumihaitirca@gmail.com (R.T.); vfilip@gmail.com (V.F.)
[3] Power Engineering Faculty; Hydraulics, Hydraulic Machines, and Environmental Engineering Department, University "Politehnica" of Bucharest, Bucharest 060042, Romania; adrian.ciocanea@yahoo.com
[4] Department of Oxide Materials and Nanomaterials, Faculty of Applied Chemistry and Material Science, University "Politehnica" of Bucharest, Bucharest 060042, Romania; eugeniuvasile@yahoo.com (E.V.)

* Correspondence: eugeniuvasile@yahoo.com (E.V.), serban@3nanosae.org (S.N.S.), Tel.: +40214574838 (S.N.S)

Received: 24 May 2020; Accepted: 16 June 2020; Published: date

1. Potential of the reference electrodes

Saturated calomel (Hg/Hg_2Cl_2), Ag/AgCl, or Hg/Hg_2SO_4 electrodes were used as reference electrodes. The experimental setup consists of an electrochemical cell with two platinum electrodes and the reference electrode [1,2]. The potential of the reference electrode was determined as the equilibrium potential ($i = 0\ mA$) for the hydrogen redox reaction:

$$2H^+(aq) + 2e^- \rightarrow H_2(g) \quad (1)$$

The electrolytes used in these measurements were 1 M HCl for Hg/Hg_2Cl_2 and Ag/AgCl and 0.5 M H_2SO_4 for Hg/Hg_2SO_4 to achieve standard conditions (pH = 1 and 1 bar H_2). The electrolytes were purged with hydrogen (hydrogen generator, Perkin Elmer—PGKH2 500) continuously throughout the experiments. The as-obtained potential for the reference electrodes is listed in Table S1 with their associated 95% confidence interval.

Table S1. The potentials of reference electrodes.

	Ag/AgCl	Hg/Hg_2Cl_2	Hg/Hg_2SO_4
Potential measured vs. SHE (mV)	199 ± 0.284	249 ± 0.281	597 ± 0.190

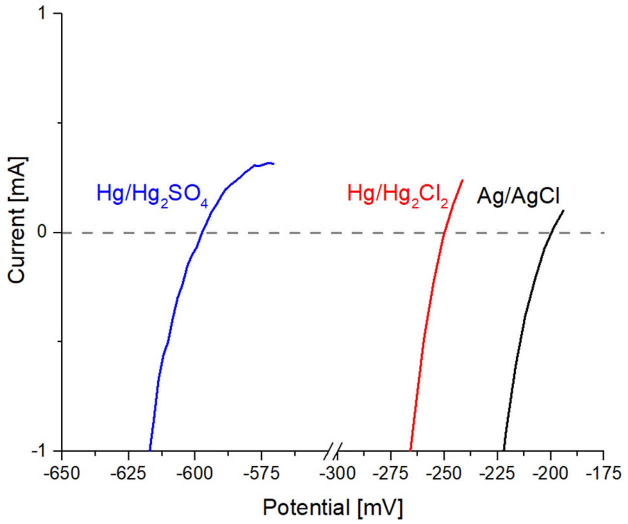

Figure S1. Measured potentials of Hg/Hg_2Cl_2, Ag/AgCl, and Hg/Hg_2SO_4.

$$E_{RHE} = E_{ref} + 59mV * pH + E^{o}_{ref} \tag{S1}$$

E_{RHE}—potential of the reversible hydrogen electrode
E_{ref}—potential of the reference electrode used in the experiment
pH—electrolyte's pH value
E^{o}_{ref}—standard potential of the electrode used in the experiment according to Table S1

2. ICP-OES Analysis

ICP-OES (Perkin Elmer, Avio 200) was used to determine the amount of platinum dissolved. The operating parameters used for ICP-OES and the selected wavelength are shown in Table S2. The wavelengths were selected by minimal interferences and high sensitivity. Pt 299.7 nm and Pt 283.0 nm [3] were eliminated because of strong interferences with Mg and Ce lines (Table S3).

Table S2. Operating parameters for ICP-OE..S

Parameter	Setting
Nebulizer Gas Flow	0.7 L/min
Auxiliary Gas Flow	0.2 L/min
RF Power	1500 W
Plasma view	Axial
Liquid sample uptake	1 mL/min
Element wavelenght (nm)	Pt 265.945 nm

Table S3. Percent interference for matrix elements of SRM 2557 in the standard resolution ICP-OES. Individual standards for each element were analyzed at Pt wavelengths at expected concentrations found in NIST SRM 2557, assuming a sample loading of 2 g into 50 mL. The ratio of interference to analyte is recorded as a percentage for each potential analyte.

Line (nm)	Ni	Ce	Al	Fe	Zr	Ba	Mg	Pb	Ca	La	Pt	Pd	Rh
Pt (265.9)								0.1	0.1				
Pt (283.0)					0.1		99						
Pt (299.7)		11					3.4						

3. Electrochemical measurements

3.1. Acidic pH

The region from –0.05 to 0.25 V versus RHE has four main peaks: two peaks on the anodic branch (positive current), which are mirrored on the cathodic branch (negative current) in 1 M HCl (inset Figure 1A). On the anodic sweep, the oxidation of molecular hydrogen can be observed by a peak centered at 0 V versus RHE and another desorption of hydrogen taking place at 0.125 V versus RHE (inset Figure 1A). The Pt peak centered at 0.125 V versus RHE decreases considerably in the last cycle in 1 M HCl (red curve inset Figure 1A). Current densities larger than 15 mA cm^{-2} are achieved at approximately 1.4 V versus RHE (i.e., 0.04 V overpotential) in 1M HCl. Such large current densities are caused by a mix between the fast two-electron chlorine evolution reaction (R4) and the slower four-electron oxygen evolution (R5).

Figure 1B shows the Pt CV in 0.5 M H_2SO_4, which is well-known and has been extensively studied. There are several features in 0.5 M H_2SO_4 in the Pt-hydride region that are caused by specific adsorption and desorption of *weakly* and *strongly* bonded hydrogen at different platinum facets. The electrochemical dissolution procedure does not significantly change the Pt features in this region. Platinum oxidation features are visible in 0.5 M H_2SO_4 from approximately 0.8 V versus RHE. Oxygen evolution (R5) is the reaction taking place in 0.5 M H_2SO_4 at potentials larger than 1.6 V versus RHE with a maximum current density of approximately 5 mA cm^{-2} at overpotentials of approximately 0.5 V. Larger current densities are obtained at a much smaller overpotential in 1 M HCl, that is, 0.04 V.

3.2. Neutral pH

Representative CVs obtained in 1 M KCl are shown in Figure 1C. Two regions are observed similar to acidic electrolytes. The oxidation of hydrogen takes place between –0.2 and 0 V versus RHE on the anodic sweep (positive currents), almost 0.2 V apart from the hydrogen desorption region. The adsorption of the hydronium and/or hydroxyl ion was observed at 0.35 V versus RHE. The desorption of hydronium and/or hydroxyl ion is found at the same potential, but on the cathodic scan. Mixed oxygen and chloride adsorption are the main features at potentials larger than 1.25 V versus RHE. Two peaks at 1.6 and 1.75 V versus RHE are clearly distinct on the cathodic scan, and were assigned to the electrochemical reduction of chlorine and oxygen, respectively. The peak at 0.5 V versus RHE in the first cycle was shifted towards 0.8 V versus RHE in the last cycle, which was assigned to the oxygen reduction reaction.

The number of peaks in 0.5 M K_2SO_4 is greater than in other electrolytes. Figure 1D shows that the hydronium and/or hydroxyl ion reduction to molecular hydrogen has a strong negative onset potential, like that observed in 1 M KCl (Figure 1C). Further on, the hydrogen desorption takes place on the anodic sweep followed by the platinum oxidation and oxygen evolution. Two peaks are observed on the cathodic sweep at 0.5 and 0.95 V versus RHE. It is widely acknowledged that the platinum oxide in neutral pH electrolyte is reduced by protons (acidic mechanism) and water (commonly observed in alkaline pH). The peak at 0.95 V versus RHE (Q1) is governed by the acidic mechanism (R7), while the peak at 0.5 V versus RHE (Q2) is believed to be proton independent (R8). The charge ratio of these two peaks (Q1/Q2) in the first cycle is 0.4, while in the last cycle, it increased to 0.95, which means that the pH at the electrode surface has turned acidic (see Supporting Material).

$$PtO + 2H^+ + 2e^- \rightarrow Pt + H_2O \quad \text{(R7)}$$

$$PtO + H_2O + 2e^- \rightarrow Pt + 2OH^- \quad \text{(R8)}$$

The change in electrode roughness was determined from the Pt-hydride region in the CVs of Figure 1 (see main body). Electrodes in K_2SO_4 have experienced an increase in the roughness factor, which can be explained by a cleaner Pt surface that is more accessible for reactions. There was no loss in roughness for electrodes in H_2SO_4. The loss in roughness was most severe in HCl and KCl, which lost 58% and 15%, respectively. The relative loss in roughness has the following trend:

$K_2SO_4 > H_2SO_4 >> KCl >> HCl$

4. Electrochemical surface area (ESA)

Two peaks are observed on the cathodic sweep at 0.3 and 0.8 V versus RHE, respectively. It is widely acknowledged that the platinum oxide in neutral pH electrolyte is reduced by protons (acidic mechanism) and water (commonly observed in alkaline pH). **Error! Reference source not found.** shows that there are two peaks: Q1 around 0.8 V versus RHE, which is governed by the acidic mechanism (R1), and Q2 around 0.3 V versus RHE, which is believed to be proton independent (R2) [**Error! Bookmark not defined.**]. The charge ratio of these two peaks (Q1/Q2) in the first cycle is 0.3, while in the last cycle, it increased to 0.95, which suggests that the electrolyte's pH has shifted to larger values.

$$PtO + 2H^{+} + 2e^{-} \rightarrow Pt + H_2O \qquad \text{(R1)}$$

$$PtO + H_2O + 2e^{-} \rightarrow Pt + 2OH^{-} \qquad \text{(R2)}$$

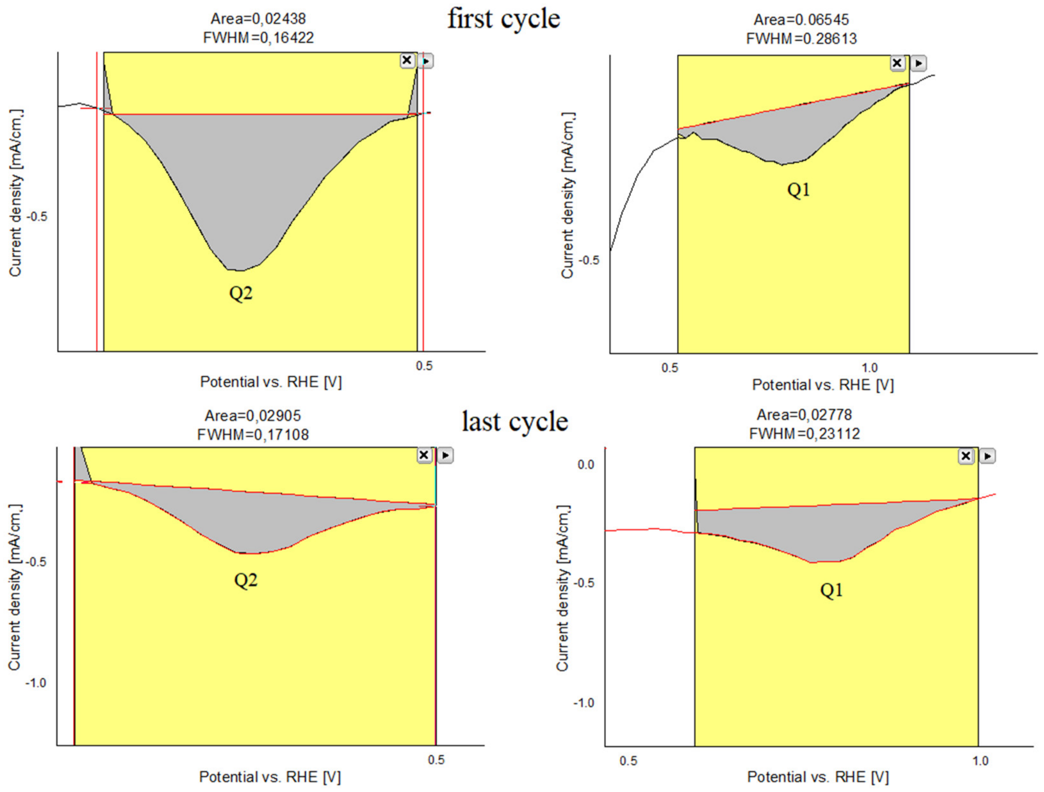

Figure S2. Calculation of electrochemical surface area for the peaks of CVs in 0.5M K_2SO_4.

5. Roughness factor

The change in electrode roughness was determined from the CVs presented in Figure 1 (from the main body of the article). The roughness factor was determined according to Equation S3.

$$r_f = \frac{ESA}{A_{geo}} = \frac{\frac{\int Q}{Q_{Pt}}}{A_{geo}} \qquad \text{(S3)}$$

r_f—roughness factor

ESA —electrochemical surface area (cm^2)

A_{geo}—geometrical area of the electrode (a disc equal to 0.785 cm^2)

Q—electrochemical charge determined by the integration of the CV in the hydride region (C)

Q_{Pt}—charge density of Pt ($C{*}cm^{-2}$)

The roughness factor at beginning-of-test (BOT) and end-of-test (EOT) for every electrolyte was determined using Equation S3. The relative roughness factor was determined using Equation S4. It is clear that the relative loss in the roughness factor (R_{rf}) is the ratio between the charge at EOT and BOT (Equation S4).

$$R_{rf}(\%) = \frac{r_{f-f}}{r_{f-i}} * 100 = \frac{\int Q_f}{\int Q_i} * 100 \tag{S4}$$

R_{rf}—relative roughness factor
$r_{f\text{-}f}$—roughness factor at EOT
$r_{f\text{-}i}$—roughness factor at BOT
Q_f—electrochemical charge determined at EOT (C)
Q_i—electrochemical charge determined at BOT (C)

Table S4. The roughness factor for electrolytes.

	R_{rf} / %
HCl	42
H_2SO_4	98
KCl	85
K_2SO_4	121

Only electrodes in K_2SO_4 have experienced an increase in the roughness factor, which can be explained by a cleaner Pt surface that is more accessible for reactions.

6. Electrochemical dissolution of platinum

Error! Reference source not found. shows the UV/vis spectra of the solutions containing platinum complexes (3.1.3 from the article). The samples in chloride electrolyte show a strong peak at 262 nm. The chemical structure of the compound was identified as [$PtCl_6$] [2–4]. The peak at 262 nm increases linearly from day 1 to day 7, which is normally because the qualitative analysis (ICP-OES) shows a linear trend during 7 days of platinum dissolution (Figure 3A from the article).

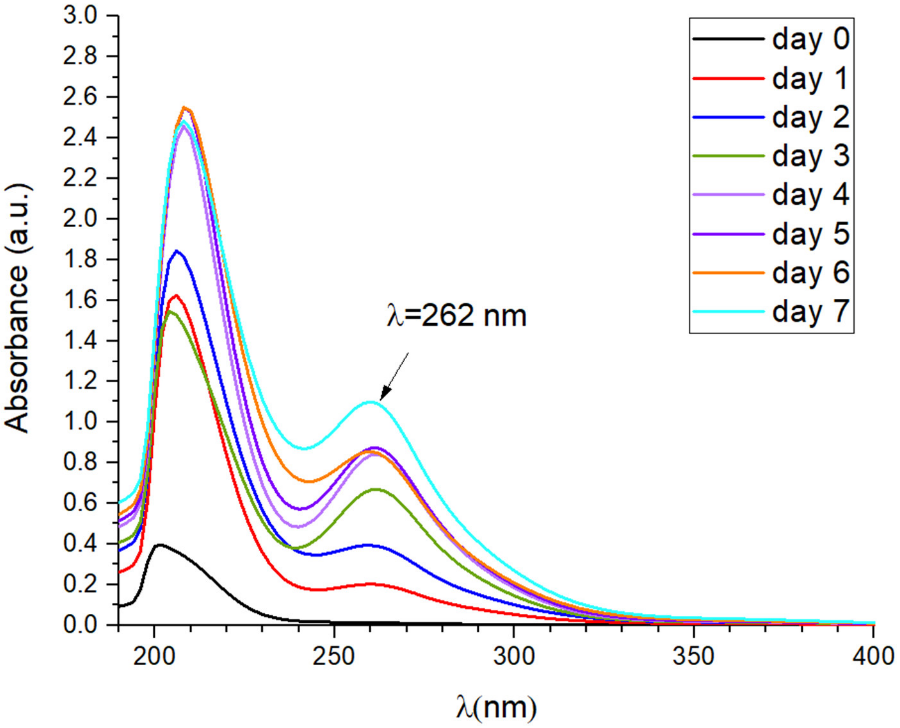

Figure S3. UV/vis spectrum of the solution from 7 days of experiment.

7. Levich equation

The mass transport can be analyzed on the basis of the Levich equation [5] (Equation S5):

$$I = 0.62\mathrm{nFAD}^{2/3}\upsilon^{-1/6}\mathrm{C}_0\omega^{1/2} \quad \text{(S5)}$$

where
I—Levich current (A)
n—number of electrons transferred
F—Faraday constant (96485 C/mol)
A—electrode area (0.0314 cm^2)
D—diffusion coefficient of chlorides ions (2.03 $\times 10^{-5}$ cm^2/s) [6]
υ—kinematic viscosity of the solution (0.089 cm^2/s)
C_0—bulk concentration of chloride in the electrolyte (1 mol/m^3)
ω—angular rotation rate (rad/s)
RPM—rotations/minute
1 RPM = 1 rotation/60 s = 2π radians/60 s = π/30 rad/s = 0.104719 rad/s

8. Preparation of solution with catalytic converter

Titanium plates were used as working electrode (8.74 cm^2) and counter electrode (11.31 cm^2) for experiments with catalytic converter. The catalyst (Figure S4A) was milled and mixed with 1M HCl for 30 minutes (Figure S4B). The obtained solution was spray coated on titanium plates (Figure S4C). The mass of catalyst was estimated by weighing the plates before and after.

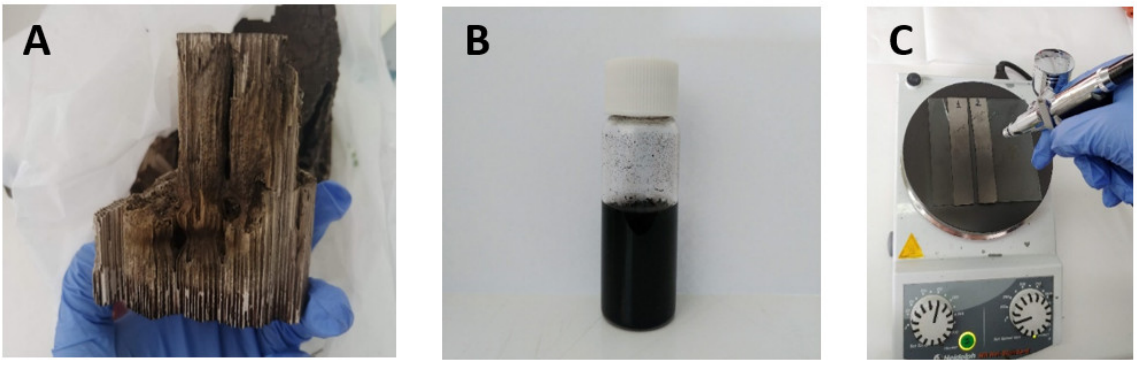

Figure S4. Preparation of solution with catalytic converter steps.

Reference:

1. Shinagawa, T.; Garcia-esparza, A.T.; Takanabe, K. Mechanistic Switching by Hydronium Ion Activity for Hydrogen Evolution and Oxidation over Polycrystalline Platinum Disk and Platinum / Carbon Electrodes. *ChemElectroChem* **2014**, *1*, 1497–1507. doi:10.1002/celc.201402085.
2. Nørgaard, C.F.; Stamatin, S.N.; Skou E.M. Redeposition of electrochemically dissolved platinum as nanoparticles on carbon, *Int. J. Hydrogen Energy*.**2014**, *39*, 17322–17326. doi:10.1016/j.ijhydene.2014.08.054.
3. Pennebaker F.M.; Denton M.B. High-precision, simultaneous analysis of Pt, Pd, and Rh in catalytic converter samples by carius tube dissolution and inductively coupled plasma atomic emission spectroscopy with charge-injection device detection, *Appl. Spectrosc*, **2001**, *55*, 504–509. doi:10.1366/0003702011952037.
4. Nørgaard C.F; Stamatin S.N; Skou E.M. Redeposition of electrochemically dissolved platinum as nanoparticles on carbon, *Int. J. Hydrogen Energy*, **2014,** *39*, 17322–17326. doi:10.1016/j.ijhydene.2014.08.054.
5. Bard, A. J.; Faulkner, L. A. Electrochemical Methods: Fundamentals and Applications, 2nd ed. *Wiley-Interscience: New York*, **2000**, p. 339
6. Cussler, E. L.; Edward Lansing Cussler. Diffusion: Mass Transfer in Fluid Systems, *Cambridge Cambridge Univ. Press* ,**2000**.